

Genotoxic Stress-Induced Cyclin D1 Phosphorylation and Proteolysis Are Required for Genomic Stability[∇]

Laura L. Pontano,^{1,2} Priya Aggarwal,¹ Olena Barbash,¹ Eric J. Brown,^{1,2}
Craig H. Bassing,^{1,3,4} and J. Alan Diehl^{1,2*}

The Abramson Family Cancer Research Institute,¹ Department of Cancer Biology,² and Department of Pathology and Laboratory Medicine,³ University of Pennsylvania, Philadelphia, Pennsylvania 19104, and Children's Hospital of Philadelphia, Philadelphia, Pennsylvania 19104⁴

Received 10 July 2008/Returned for modification 28 July 2008/Accepted 14 September 2008

While mitogenic induction of cyclin D1 contributes to cell cycle progression, ubiquitin-mediated proteolysis buffers this accumulation and prevents aberrant proliferation. Because the failure to degrade cyclin D1 during S-phase triggers DNA rereplication, we have investigated cellular regulation of cyclin D1 following genotoxic stress. These data reveal that expression of cyclin D1 alleles refractory to phosphorylation- and ubiquitin-mediated degradation increase the frequency of chromatid breaks following DNA damage. Double-strand break-dependent cyclin D1 degradation requires ATM and GSK3 β , which in turn mediate cyclin D1 phosphorylation. Phosphorylated cyclin D1 is targeted for proteasomal degradation after ubiquitylation by SCF^{Fbx4- α Bcrystallin}. Loss of Fbx4-dependent degradation triggers radio-resistant DNA synthesis, thereby sensitizing cells to S-phase-specific chemotherapeutic intervention. These data suggest that failure to degrade cyclin D1 compromises the intra-S-phase checkpoint and suggest that cyclin D1 degradation is a vital cellular response necessary to prevent genomic instability following genotoxic insult.

Mitogenic signals coordinated by the small GTP binding protein Ras induce D-type cyclin expression during G₁ phase of the cell cycle. Active cyclin D1/cyclin-dependent kinase 4 (CDK4) complexes accumulate in the nucleus, triggering G₁ progression via phosphorylation-dependent inactivation of the retinoblastoma protein (Rb) and related pocket proteins (14, 22, 23, 35). The cyclin D1/CDK4 kinase also facilitates activation of cyclin E/CDK2 through titration of the CDK inhibitors p21^{Cip1} and p27^{Kip1}, contributing to Rb phosphorylation by the cyclin E/CDK2 kinase (45).

After the G₁/S transition, cyclin D1 activation is terminated by glycogen synthase kinase 3 β (GSK3 β)-dependent threonine-286 (Thr-286) phosphorylation, which triggers CRM-1-dependent nuclear export and ubiquitin-mediated proteolysis (17). Proteolytic inactivation is essential since cyclin D1 synthesis does not decrease in the presence of continuous growth factor signaling (40). Cytoplasmic Thr-286 phosphorylated cyclin D1 is targeted for degradation via the SCF^{Fbx4- α Bcrystallin} E3 ubiquitin ligase, and recognition of phosphorylated cyclin D1 is mediated by both Fbx4 and α B crystallin (36).

Of the numerous cell cycle regulatory proteins, cyclin D1 is one of the most frequently targeted in human cancer, with overexpression resulting from gene amplification, chromosomal translocation, and protein stabilization (45). Cyclin D1 overexpression has been observed in various malignancies, including carcinomas of the breast, esophagus, colon, and lung (5, 7–9, 26, 28). While cyclin D1 overexpression occurs at a significant frequency, overexpression per se is insufficient to

drive neoplastic transformation. In contrast, cyclin D1 mutants that are refractory to Fbx4-dependent proteolysis and accumulate in the nucleus are acutely transforming (3, 21, 37). Consistent with disruption of cyclin D1 proteolysis functioning as an agonist of neoplastic growth, mutations that disrupt cyclin D1 nuclear export and thus, ubiquitin-mediated proteolysis, have been identified in human cancers (10, 41). In addition, recent screening of human esophageal tumor samples revealed inactivating mutations in Fbx4, which will again drive nuclear cyclin D1 accumulation (4).

Genomic instability is a hallmark of human cancers implicated in initiation and promotion of tumorigenesis. Double-strand DNA breaks (DSBs) arise following gamma-irradiation (γ IR) or destabilization of stalled replication forks; checkpoint kinases respond to such lesions, promoting cell cycle arrest and DNA repair (30). Impaired detection or repair of DSBs results in chromosomal translocations and deletions, triggering genomic instability (31). The intra-S-phase checkpoint responds to DSB induction occurring at loci outside actively replicating DNA; failure to reduce the rate of DNA synthesis after such genotoxic insult results in radioresistant DNA synthesis (RDS), a phenotype associated with abrogated checkpoint signaling through ATM (ataxia-telangiectasia mutated) and downstream effectors (6). The primary mechanism of DSB-induced S-phase arrest involves inhibition of unfired replication origins (6, 16, 19).

Recent evidence revealed that ubiquitylation refractory cyclin D1 accumulates as an active D1/CDK4 kinase within the nucleus during S-phase, where it promotes DNA rereplication, thereby linking cyclin D1 deregulation with S-phase perturbation (2). Previous work implicated cyclin D1 destruction following DNA damage in promoting G₁-phase cell cycle arrest (1). Consequently, we have investigated the role of cyclin D1 degradation for genomic stability following genotoxic stress. The data provided reveal that cyclin D1 is rapidly degraded in

* Corresponding author. Mailing address: The Abramson Family Cancer Research Institute, Department of Cancer Biology, 454 BRB II/III, 421 Curie Boulevard, Philadelphia, PA 19104-6140. Phone: (215) 746-6389. Fax: (215) 746-5511. E-mail: adiehl@mail.med.upenn.edu.

[∇] Published ahead of print on 22 September 2008.

a phosphorylation-dependent manner after DSB induction, and failure to degrade cyclin D1 compromises the intra-S-phase checkpoint response. Furthermore, evidence is provided revealing that ATM signaling is critical for GSK3 β -dependent cyclin D1 phosphorylation, highlighting the relevant signaling pathway that coordinates DSB induction with cyclin D1 regulation.

MATERIALS AND METHODS

Cell Culture Conditions. NIH 3T3, MDA-MB 231, MCF7, U20S, ATR^{fllox/-} CET immortalized ear fibroblasts, and 293T cells were maintained in complete Dulbecco modified Eagle medium (Cellgro) containing glutamine, 1% penicillin-streptomycin (Cellgro), and 10% fetal bovine serum (FBS; Gemini Bioproducts); MDA-MB 231 and MCF7 cells were also supplemented with 10 μ g of insulin (Gibco)/ml. KYSE 520 and TE3/TE7 cells were maintained in RPMI medium (Gibco) containing glutamine, antibiotics, and 10% FBS. NIH 3T3 cells stably expressing FLAG-D1, FLAG-D1T286A, FLAG-D1290-95A, α B crystallin short hairpin RNA (shRNA), and Fbx4 shRNA have been previously described (10, 18, 36). Acute ATR deletion was achieved by treating cells with 200 nM 4-OH tamoxifen for 24 h, followed by incubation for an additional 12 h to allow efficient depletion. For transient expression, cells were transfected by using Lipofectamine (Invitrogen). For synchronization, NIH 3T3 cells and their derivatives were cultured in media containing 0.1% FBS for 24 h, followed by the addition of FBS for 15 h for a synchronous S-phase population, as determined by fluorescence-activated cell sorting (FACS). Genotoxic stress was induced by γ IR using a ¹³⁷Cs source (MS Nordion Gammacell 40 Exactor), 2 mM hydroxyurea (HU; Sigma), 10 or 20 μ g of bleomycin (Sigma)/ml, or 5 μ M aphidicolin (Sigma). For proteasome inhibition experiments, cells were treated with 10 μ M MG132 (Calbiochem) and 2 mM HU for 4 h. The following small-molecule inhibitors were used according to the manufacturer's recommendation: GSK3 β inhibitors LiCl (Sigma) and SB216763 (Calbiochem) and p38 inhibitor SB203580 (Calbiochem). The cells were pretreated with inhibitors for 30 min prior to DNA damage induction. For ATM inhibition, the cells were pretreated with KU-55933 (Sigma) for 30 min. For Chk1 or Chk2 inhibition, the cells were pretreated with SB218078 (Calbiochem) or Chk2 inhibitor II (Sigma) for 30 min, followed by DNA damage. The pJ3M-kdGSK3 β construct was described previously (17). Chromatin fractionation was performed as described previously (20).

Cell cycle analysis. NIH 3T3 cells stably expressing cyclin D1 or D1T286A were treated with chemotherapeutic agent camptothecin (CPT) for 24 or 48 h. Cells were washed with phosphate-buffered saline, fixed with ethanol, and stained with propidium iodide for 30 min, prior to FACS analysis. Cell cycle profiles based on DNA content were established by using FlowJo software, and the sub-G₁ population of cells served as a readout for apoptotic cells following CPT treatment in three independent experiments.

Immunoblotting. Cells were lysed in Tween 20 buffer containing protease and phosphatase inhibitors (50 mM HEPES [pH 8.0], 150 mM NaCl, 2.5 mM EGTA, 1 mM EDTA, 0.1% Tween 20, 1 mM dithiothreitol [DTT], 0.1 mM phenylmethylsulfonyl fluoride, 20 U of aprotinin/ml, 10 mM β -glycerophosphate, 5 μ g of leupeptin/ml, and 1 mM NaF). M2 Agarose beads were utilized to precipitate Flag-tagged protein in Tween 20 buffer. Antibodies used for direct Western include cyclin D1-72-13G, R2 (phospho-T286), cyclin D2, cyclin E, CDK4, myc 9E10 (Santa Cruz), γ -H2AX, phospho-p38, Chk1, phospho-p53 (Ser 15), phospho-ATM (Cell Signaling), ATM, ATR (Serotec), Chk2, GSK3 β (BD Transduction Labs), β -actin (AC15; Sigma), α B crystallin (SPA 223; Stressgen), and Fbx4 (Rockland Immunochemicals).

In vitro kinase assay. An equal concentration of endogenous GSK3 β was precipitated from NIH 3T3 cells that were untreated or subjected to γ IR using protein A-Sepharose beads in GSK3 β immunoprecipitation buffer (50 mM Tris-HCl [pH 7.5], 1 mM EDTA, 1 mM EGTA, 10% Triton X-100, 0.27 M sucrose, 1 mM DTT, and protease/phosphatase inhibitors). GSK3 β -bound beads were washed with kinase buffer (20 mM Tris-HCl, 40 mM MgCl₂, 2.5 mM EGTA, 1 mM DTT, protease/phosphatase inhibitors, and 20 μ M ATP). Reactions were carried out in the presence of [γ -³²P]ATP for 20 min at 30°C, resolved by sodium dodecyl sulfate-polyacrylamide gel electrophoresis, and transferred to a nitrocellulose membrane. Immunoblotting for GSK3 β indicated equal precipitation of kinase, and a normal rabbit serum precipitation served as a negative control.

Metaphase spreads. Splenocytes were isolated from transgenic E μ -D1T286A or nontransgenic control mouse spleens and cultured for 48 h in RPMI medium supplemented with L-glutamine, lipopolysaccharide, β -mercaptoethanol, concanavalin A, and FBS. Cultures were treated with 100 μ M mitomycin C (MMC)

for 24 h to induce damage. For HU experiments, cultures were treated for 2 h with 2 mM HU, washed, and resuspended in fresh media. Cells were arrested in metaphase by treatment with Colcemid (Gibco) for 2 h. Cells were treated with hypotonic KCl solution and fixed with methanol-acetic acid. Metaphase spreads were dropped, permitted to dry overnight, and then stained with Giemsa (Sigma). The average number of chromatid breaks per cell was scored in 16 metaphase spreads following HU treatment or 25 total spreads for MMC treatment. NIH 3T3 cells expressing vector control, Fbx4shRNA, or cyclin D1T286A were synchronized by serum starvation and treated with 2 mM HU for 3 h during S phase, followed by 4 h of 0.5 μ M nocodazole treatment to arrest cells in metaphase. Metaphase spreads were prepared as described for splenocytes, and chromatid breaks in 20 metaphases for each treatment were scored in a blind fashion.

RDS assays. Cells were synchronized by serum starvation for 24 h in the presence of 20 nCi of [¹⁴C]thymidine (Amersham). Cells were subsequently washed with phosphate-buffered saline, and Dulbecco modified Eagle medium containing 10% serum was added to trigger entry into S phase. S-phase populations were exposed to 10 Gy of γ IR as indicated, followed by a recovery period at 37°C for 30 min. Cells were then pulsed with 20 μ Ci of [³H]thymidine (Perkin-Elmer) for 2 h, and total DNA was isolated by high-salt extraction. Equal concentrations of purified DNA were subjected to scintillation counting, and DNA synthesis was expressed as the ratio of [³H]/[¹⁴C] incorporation, normalized to nonirradiated (control) cells.

shRNA/siRNA. Luciferase control and Chk2-specific small interfering RNAs (siRNAs; Dharmacon Smartpool) were kindly provided by Roger Greenberg, University of Pennsylvania. ATR-specific siRNA Smartpool was purchased from Dharmacon. siRNAs were transfected into U20S cells by using HiPerfect (Qiagen). Cells were irradiated at 60 h after siRNA transfection and harvested for Western blotting. For Chk1 shRNA experiments, scramble control or Chk1.1 shRNA lentivirus (pLKO.1 vector) were used to infect NIH 3T3 cells. At 72 h postinfection, the cells were plated and synchronized by serum starvation. Cells were released into complete media, and after 15 h the cells were treated with HU to induce replication stress in S phase.

Statistical analysis. Error bars indicate mean \pm the standard deviation. The Student *t* test was used to compare groups in RDS assays, metaphase spread analysis, and sensitivity to CPT assays. Western blotting quantification was performed by densitometric analysis. Error bars indicate means \pm the standard deviations of the densitometry of three independent experiments.

RESULTS

Expression of ubiquitylation refractory cyclin D1T286A generates chromosomal instability following DNA damage. Transgenic mice expressing cyclin D1T286A driven by the E μ enhancer develop B-cell lymphomas with significant aneuploidy and chromosomal translocations (2). Because cyclinD1T286A is refractory to ubiquitin-mediated proteolysis (18), we determined whether its expression also compromised genomic integrity in response to transient exposure to DNA-damaging agents. Nonmalignant splenocytes derived from E μ -D1T286A mice that were exposed to MMC exhibited a significant increase in chromatid breaks relative to nontransgenic controls (Fig. 1A). Similarly, exposure to HU increased the incidence of chromatid breaks in D1T286A-expressing cells compared to nontransgenic controls (Fig. 1B). Importantly, untreated nontransgenic and E μ -D1T286A splenocytes exhibited infrequent chromatid breaks (Fig. 1C), indicating synergy between cyclin D1T286A and DNA damage in promoting genomic instability.

DSBs trigger phosphorylation-dependent cyclin D1 degradation. The enhanced frequency of chromatid breaks in cells expressing cyclin D1T286A might reflect the refractory nature of this allele to proteasome-dependent destruction (18). In fact, genotoxic stress normally triggers the rapid loss of cyclin D1, which has been attributed to ubiquitin-mediated destruction during G₁ phase (1). Based on these findings, we investigated the mechanism governing cyclin D1 loss following S-phase DNA damage. NIH 3T3 cells were treated with HU, a

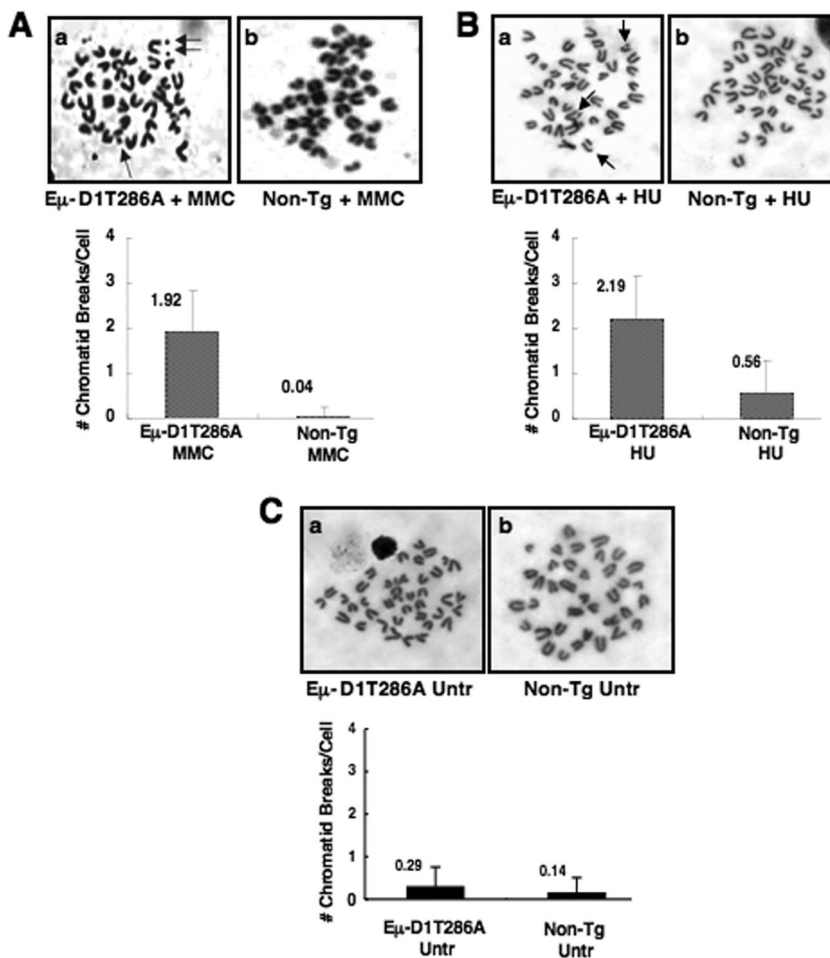


FIG. 1. (A and B) Chromatid breaks following MMC (A) or HU (B) treatment occur at a greater frequency in splenocytes expressing Eμ-D1T286A. Splenocytes derived from nontransgenic or pre-malignant Eμ-D1T286A mice were cultured for 24 h in the presence of 100 μM MMC or cultured for 24 h, followed by a 2-h pulse with 2 mM HU and resuspension in fresh media. Cells were then treated with Colcemid for 2 h to allow arrest in metaphase. (C) Untreated nontransgenic and Eμ-D1T286A splenocytes do not exhibit a significant number of chromatid breaks. Representative images of metaphase spreads are shown, and the average number of chromatid breaks per metaphase spread was quantified for each treatment.

compound that stalls DNA replication by depleting nucleotide pools and generates double breaks as a consequence of replication fork collapse (12, 39). HU treatment promoted a rapid decline in both endogenous cyclin D1 protein and exogenously expressed, Flag-tagged cyclin D1 (Fig. 2A; data not shown). Cyclin D1 mRNA levels remained constant, a finding consistent with posttranslational regulation (data not shown). We subsequently assessed cyclin D1 loss at varied HU concentrations. Cyclin D1 loss was readily apparent by 0.5 mM HU and was maximal at 1 to 2 mM HU (Fig. 2A); an intermediate dose of 2 mM was selected for analysis.

We next determined whether proteasome-resistant, non-phosphorylatable D1T286A was refractory to DNA damage-dependent downregulation. NIH 3T3 cells stably expressing equivalent levels of either wild-type Flag-D1 (3T3-D1) or Flag-D1T286A (3T3-D1T286A) were utilized (18). Treatment of cells synchronously proliferating through S phase with 2 mM HU triggered the loss of wild-type cyclin D1 protein; this loss was inhibited by concurrent application of MG132, revealing proteasome dependence (Fig. 2B). In contrast, D1T286A lev-

els were constant following HU treatment (Fig. 2B and C). If accelerated loss of cyclin D1 is determined by increased proteolysis, the cyclin D1 half-life should decrease following DNA damage. S-phase NIH 3T3 cells were left untreated or treated with 2 mM HU for 30 min, followed by the addition of cycloheximide. Western analysis revealed that the cyclin D1 half-life was reduced following HU compared to untreated cells (Fig. 2D). These results support a model wherein DNA damage induced by HU triggers phosphorylation- and proteasome-dependent degradation of cyclin D1.

We then ascertained whether cyclin D1 proteolysis required the generation of DSBs. Asynchronously proliferating 3T3-D1 or 3T3-D1T286A cells were subjected to 10Gy γIR, and cyclin D1 levels were assessed by immunoblotting. IR, like HU, triggered the rapid loss of wild-type cyclin D1 but not D1T286A (Fig. 2E). Similar to IR, bleomycin treatment also induced rapid, phosphorylation-dependent destruction of cyclin D1 (Fig. 2F), implying that DSBs promote cyclin D1 degradation. To directly address whether stalled DNA replication without DSB induction can trigger cyclin D1 destruction with similar

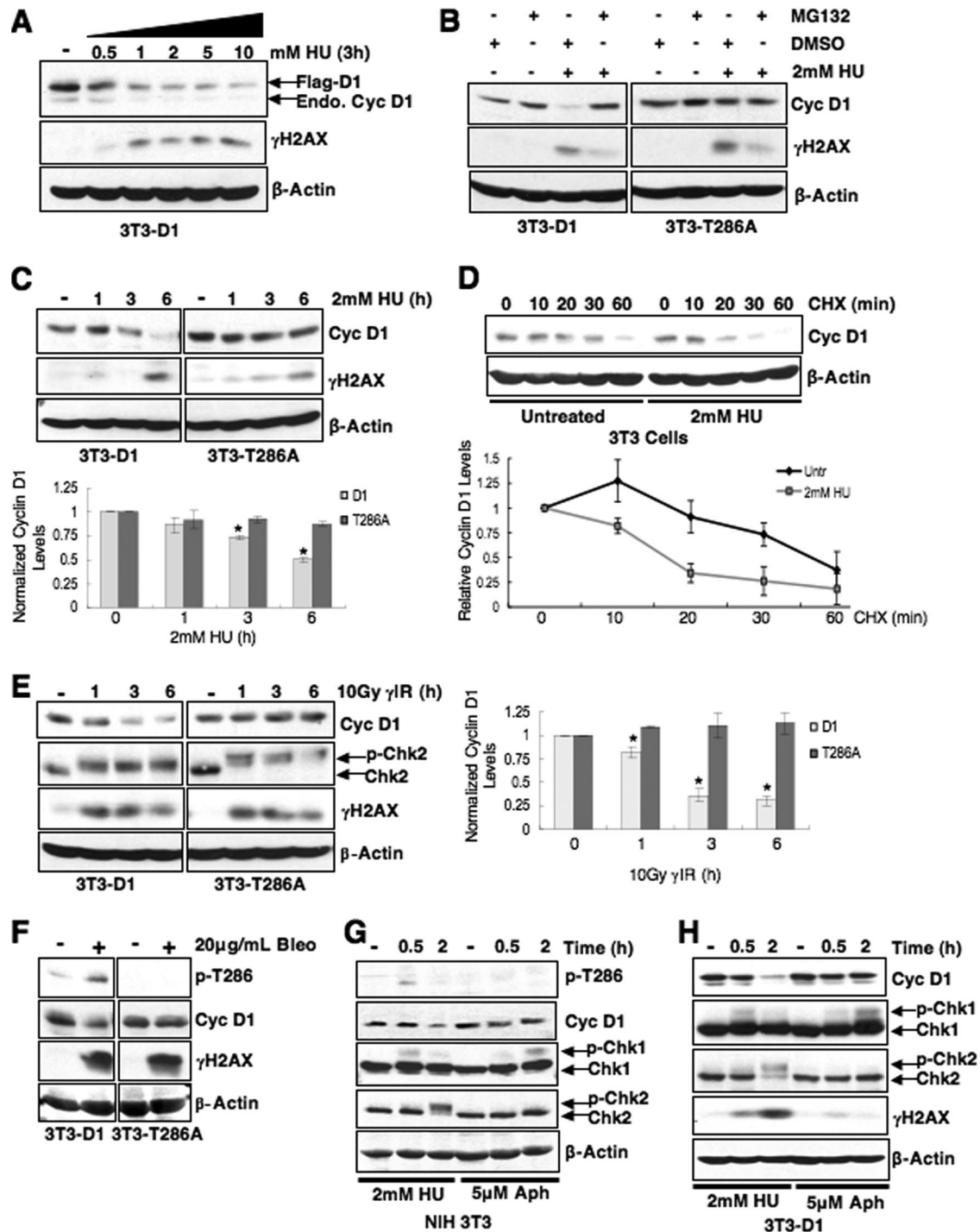


FIG. 2. Phosphorylation-dependent proteolysis of cyclin D1 following DSB induction. (A) Cyclin D1 is degraded following replication stress. Synchronous 3T3-D1 cells were treated with increasing doses of HU as indicated, and cell lysates were probed for cyclin D1 and γ H2AX as a marker of DSB induction. The 2 mM dose was selected for further HU experiments. (B and C) Cyclin D1 degradation is phosphorylation and proteasome dependent. (B) Synchronous 3T3-D1- or 3T3-D1T286A-expressing cells were treated with MG132 and HU for 4 h; immunoblots were performed as in panel A. (C) 3T3-D1 or D1T286A cells were treated with HU as indicated, and cyclin D1 levels were assessed. (D) HU treatment decreases cyclin D1 $t_{1/2}$. S-phase NIH 3T3 cells were pretreated with HU, followed by 100 μ g of cycloheximide (CHX)/ml as indicated, and cyclin D1 protein levels were assessed. (E) Cyclin D1 levels rapidly decline following γ IR. 3T3-D1 or 3T3-D1T286A cells were subjected to 10Gy γ IR, and cyclin D1 levels were assessed. Chk2 mobility shift (upper band) and γ H2AX served as markers of DSBs. (F) The DSB-inducing agent bleomycin promotes cyclin D1 degradation. Asynchronous 3T3-D1 or D1T286A cells were treated with 20 μ g of bleomycin (Bleo)/ml for 2 h, and the cyclin D1 levels were assessed. (G and H) Stalled DNA replication is not sufficient to induce cyclin D1 proteolysis. Synchronous NIH 3T3 cells (G) or NIH 3T3 cells stably expressing ectopic cyclin D1 (H) were treated with 2 mM HU to induce DSBs or 5 μ M aphidicolin (Aph) to stall DNA replication without inducing DNA breaks. Immunoblot for Chk1 mobility shift served as a marker of stalled replication, and a Chk2 mobility shift indicates DSB induction. Cyclin D1 is phosphorylated (G) and degraded (G and H) following DSB induction.

kinetics as observed with DSB-inducing treatments, cyclin D1 stability was compared for aphidicolin and HU treatment. NIH 3T3 or 3T3-D1 cells were synchronized by serum starvation for 24 h and serum stimulated for 15 h to enter S phase; cells were then subjected to short-term, low-dose aphidicolin treatment to promote the accumulation of single-strand DNA without collapsing replication forks (38) or 2 mM HU, previously shown to induce cyclin D1 degradation (Fig. 2A to D). A significant percentage (>80%) of cells were in S phase throughout the duration of treatment with DNA-damaging agents as determined by flow cytometry (data not shown). In contrast to HU or γ IR, both endogenous and ectopic cyclin D1 levels remained stable following aphidicolin treatment (Fig. 2G and H). Significantly, cyclin D1 is only phosphorylated in a damage-dependent manner after HU treatment (Fig. 2G), a finding consistent with activation of Chk2 signaling as an indicator of DSB induction. Chk1 is activated following both aphidicolin and HU treatment, which is consistent with stalled replication; however, a mobility shift in Chk2 due to ATM-dependent phosphorylation was not observed in aphidicolin-treated cells, indicating that this treatment fails to activate the ATM pathway (Fig. 2G). Collectively, these data demonstrate that stalled replication is not sufficient to induce cyclin D1 loss despite activation of the ATR (ATM and Rad3-related)-Chk1 DNA damage response pathway.

To ensure that the stability of D1T286A was not a reflection of ectopic expression, we also examined cyclin D1 response to DSB in human tumor-derived cells harboring either wild-type D1 (KYSE520) or an analogous endogenous cyclin D1P287A (TE3/7) allele (11). KYSE520 cells exhibited rapid cyclin D1 degradation following γ IR, while cyclin D1P287A, expressed in TE3 and TE7 cells, was refractory to degradation after a moderate or high γ IR dose (Fig. 3A and B). Cyclin D2 and cyclin E degradation was not triggered by irradiation, an observation consistent with previous work indicating that DNA damage-induced regulation is restricted to cyclin D1 (1) (Fig. 3C). Collectively, our data suggest that bona fide DNA breaks are a prerequisite for cyclin D1-specific proteolysis in response to DNA damage.

GSK3 β catalyzes cyclin D1 threonine 286 phosphorylation following genotoxic stress. The stability of D1T286A to DSB-mediated destruction suggests that phosphorylation of this residue is essential for genotoxic stress-induced cyclin D1 loss. If so, genotoxic stress should trigger increased Thr-286 phosphorylation (p-T286). Indeed, both irradiation (Fig. 4A) and bleomycin (Fig. 2F) triggered an increase in p-T286 prior to cyclin D1 proteolysis. Because the cyclin D1 E3 ligase is cytoplasmic, ubiquitin-mediated proteolysis requires both p-T286 and cytoplasmic redistribution (3, 18, 36). If genotoxic stress utilizes the same machinery to eliminate cyclin D1, then nuclear export-deficient cyclin D1 mutants should accumulate as p-T286 proteins in the nucleus. To test this notion, we examined the regulation of cyclin D1-290/95A, a cyclin D1 mutant harboring an inactive nuclear export sequence, but retaining the GSK3 β phosphorylation site (10). Consistent with our hypothesis, D1-290/95A was resistant to DSB-dependent proteolysis and accumulated as a phosphorylated protein (Fig. 4A, right panel).

GSK3 β catalyzes phosphorylation of Thr-286 at the G₁/S boundary to promote cyclin D1 loss (17). To determine whether GSK3 β mediates DSB-dependent Thr-286 phosphor-

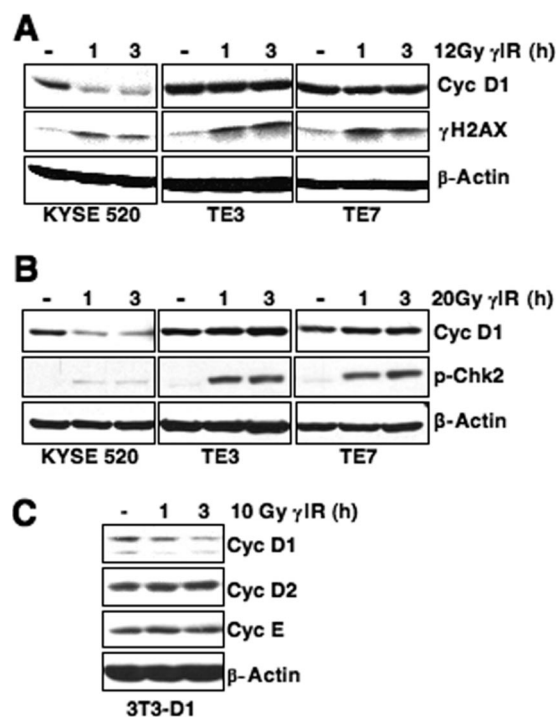


FIG. 3. IR-induced degradation is specific to wild-type cyclin D1 protein. (A and B) Cyclin D1 is refractory to degradation in esophageal carcinoma cells harboring the endogenous P287A mutation. Asynchronously proliferating cells expressing wild-type cyclin D1 (KYSE 520) or P287A mutant cyclin D1 (TE3/TE7) were irradiated with a moderate dose (A) or high dose (B), and cyclin D1 levels and checkpoint activation were assessed by immunoblotting as indicated. (C) Cyclin D1, but not cyclin D2 or cyclin E, is degraded following DNA damage. Asynchronously proliferating NIH 3T3 cells stably expressing cyclin D1 were irradiated, followed by recovery at 37°C. Protein stability was assessed by direct Western blotting.

ylation, we initially utilized a kinase-dead GSK3 β (kdGSK3 β) allele. Cyclin D1 phosphorylation was assessed 20 min after γ IR in order to visualize this highly labile protein in the absence of proteasome inhibition; importantly, significant cyclin D1 degradation is not evident at this early time following DNA damage in NIH 3T3 cells (Fig. 2G and H). Expression of kdGSK3 β attenuated Thr-286 phosphorylation following γ IR (Fig. 4B). As an independent assessment of GSK3 β dependence, NIH 3T3 cells were treated with LiCl (46) or a small molecule inhibitor of GSK3 β , SB216763. Both inhibitors also attenuated cyclin D1 phosphorylation following γ IR (Fig. 4C). As a third method for assessing GSK3 β -dependent Thr-286 phosphorylation, shRNA technology was utilized to attenuate GSK3 β expression. 293T cells were transfected with vectors encoding cyclin D1 and CDK4 along with control or GSK3 β -specific shRNA. Immunoblotting confirmed a reduction in GSK3 β protein levels (Fig. 4D). Attenuation of GSK3 β expression significantly reduced cyclin D1 phosphorylation compared to control shRNA-transfected cells (Fig. 4D). Collectively, three independent methods GSK3 β inhibition reveal that this kinase regulates Thr-286 phosphorylation following DNA damage.

Since cyclin D1 is rapidly phosphorylated following DNA damage, we determined whether GSK3 β kinase activity was

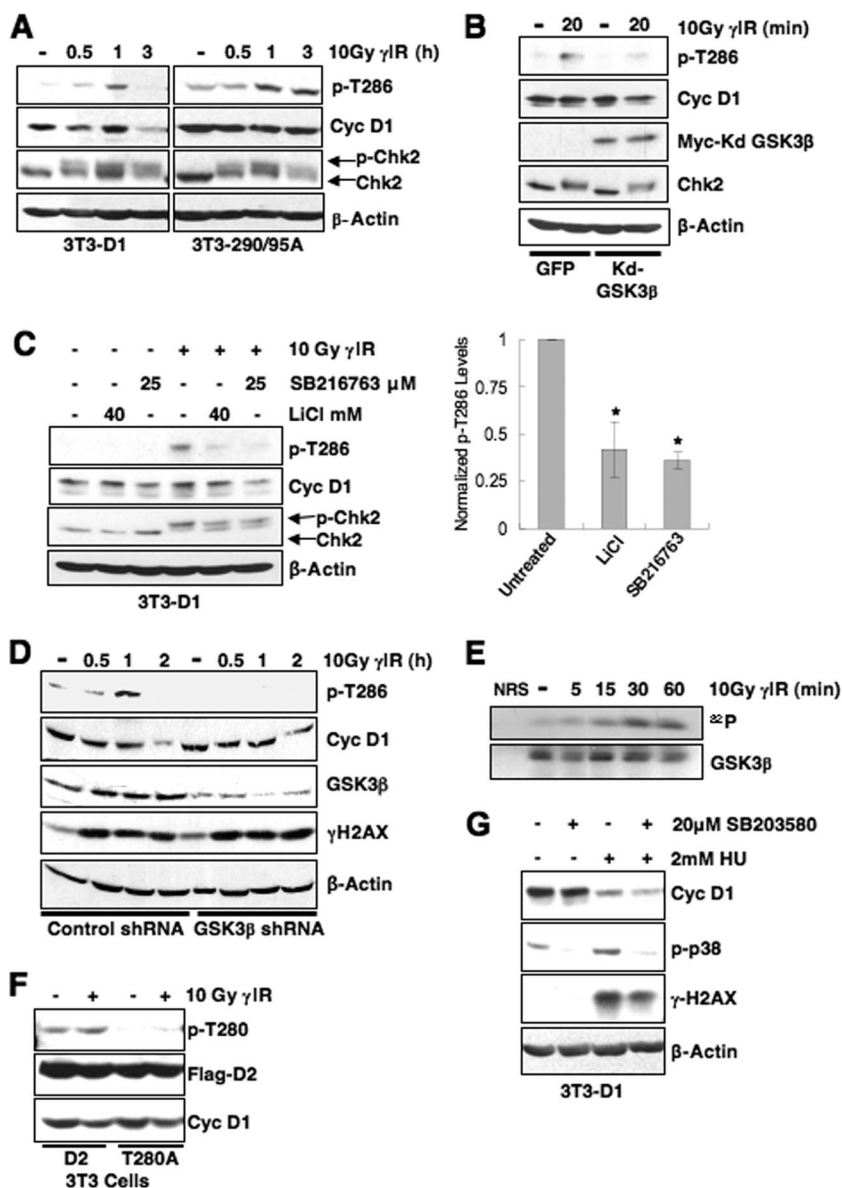


FIG. 4. GSK3 β catalyzes rapid cyclin D1 T286 phosphorylation following DNA damage. (A) Cyclin D1 phosphorylation is induced by DNA damage. Asynchronous 3T3-D1, 3T3-D1-290/95A, or 3T3-D1T286A were subjected to γ IR, and immunoblots were performed with antibodies specific to p-T286, cyclin D1, and γ H2AX. (B) Expression of kdGSK3 β abrogates cyclin D1 phosphorylation following γ IR. Lysates NIH 3T3 cells transiently expressing green fluorescent protein (GFP) or kdGSK3 β plus GFP and γ -irradiated were blotted for p-T286, cyclin D1, and myc to detect myc-tagged kdGSK3 β . (C) Inhibition of GSK3 β attenuates cyclin D1 phosphorylation following DNA damage. 3T3-D1 cells were pretreated with the GSK3 β inhibitor LiCl or SB216763, followed by γ IR and recovery for 30 min. Cyclin D1 phosphorylation was assessed by immunoblot for p-T286 and total cyclin D1. Chk2 mobility shift and γ H2AX indicate DSB induction. (D) shRNA-mediated knockdown of GSK3 β attenuates cyclin D1 phosphorylation. 293T cells were transfected with control or GSK3 β -specific shRNA, cyclin D1, and CDK4 constructs. Cells were subjected to γ IR and recovery for the times indicated, and cyclin D1 phosphorylation, efficiency of GSK3 β knockdown, and checkpoint activation were assessed by immunoblotting. (E) GSK3 β is activated following DNA damage. Endogenous GSK3 β precipitated from cells following γ IR was utilized as a kinase for *in vitro* reactions with recombinant myelin basic protein substrate. (F) Cyclin D2 Thr-280 phosphorylation is not induced following DNA damage. NIH 3T3 cells were transiently transfected with wild-type or D2T280A. Cells were irradiated 48 h posttransfection; cyclin D2 phosphorylation was assessed by Western blotting, and probing for total flag-tagged cyclin D2 served as a loading and transfection control. (G) Cyclin D1 is rapidly degraded following DNA damage in the presence of p38 inhibitor. Synchronous NIH 3T3 cells were pretreated with 20 μ M SB203580 or DMSO for 30 min, followed by HU treatment for 2.5 h. Cell lysates were prepared and probed for p-p38 and cyclin D1.

increased following γ IR. Previously published work revealed an increase in GSK3 β kinase activity after UV irradiation (34). GSK3 β immunoprecipitation-kinase reactions from irradiated NIH 3T3 cells revealed increased GSK3 β kinase activity following γ IR (Fig. 4E).

GSK3 β can also phosphorylate cyclin D2 on threonine-280 (Thr-280) during an asynchronous cell cycle and thereby trigger its proteasome-dependent loss (32). Consequently, we determined whether cyclin D2 phosphorylation was regulated by γ IR. Cyclin D2 Thr-280 phosphorylation was not induced

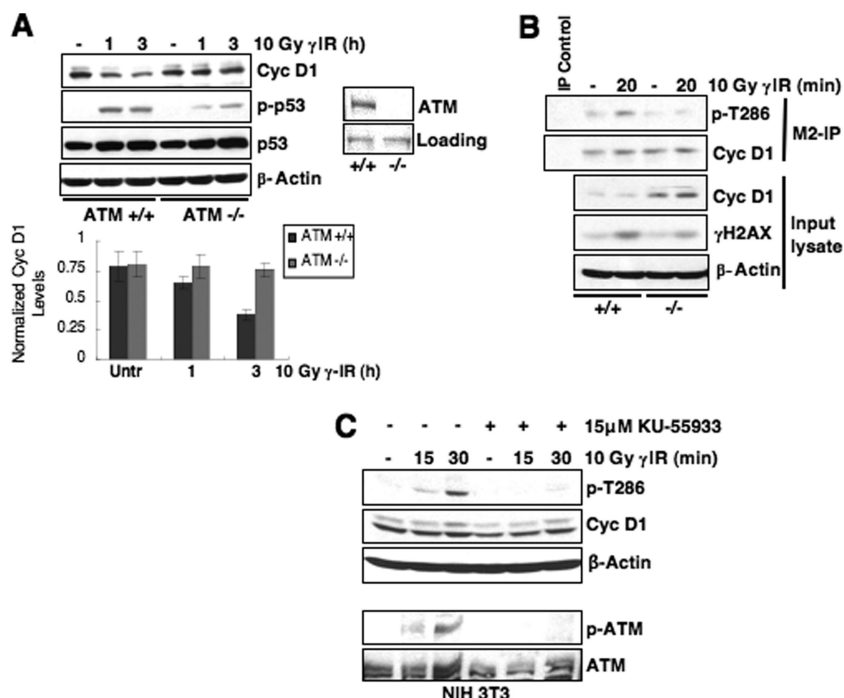


FIG. 5. ATM signaling is required for cyclin D1 phosphorylation following DSB induction. (A) Cyclin D1 degradation is attenuated in cells lacking ATM expression. Immortalized $ATM^{+/+}$ or $ATM^{-/-}$ mouse embryonic fibroblasts (MEFs) expressing Flag-tagged cyclin D1 were gamma irradiated, and cyclin D1 levels were assessed. p-p53/total p53 induction served as markers of checkpoint activation in these cell lines. (B) DNA damage-induced cyclin D1 phosphorylation is only detected in cells expressing ATM. Immortalized $ATM^{+/+}$ or $ATM^{-/-}$ MEFs expressing Flag-tagged cyclin D1 were irradiated as indicated, and lysates were precipitated with M2-agarose to detect Flag-tagged protein. Cyclin D1 phosphorylation and total levels were assessed by immunoblotting. (C) ATM signaling is required for cyclin D1 phosphorylation. NIH 3T3 cells were pretreated with DMSO or the specific ATM inhibitor KU-55933 for 30 min, followed by γ IR and recovery for 15 or 30 min. Phosphorylated and total cyclin D1 were detected by immunoblotting. A second Western blot was performed with these lysates to probe for phosphorylated ATM and total ATM to ensure efficacy of ATM inhibition.

above basal levels following γ IR (Fig. 4F). This finding suggests that while GSK3 β kinase activity is increased following DNA damage, additional regulatory mechanisms exist to allow GSK3 β -dependent cyclin D1 phosphorylation specifically. A second kinase, p38^{SAPK}, has been implicated in stress-induced cyclin D1 phosphorylation (15), and DNA damage increases p38^{SAPK} activity (44). We therefore determined whether p38^{SAPK} contributes to DNA damage-dependent cyclin D1 destruction. Significantly, p38 inhibition did not stabilize cyclin D1 protein, suggesting that p38 is not a key regulator of DSB-induced cyclin D1 loss (Fig. 4G). Collectively, these results indicate that GSK3 β is the primary kinase responsible for DSB-dependent cyclin D1 phosphorylation.

ATM signaling coordinates DSB induction with cyclin D1 phosphorylation. Because the ATM kinase is the primary signal transducer following DSB induction, we determined whether either ATM or the related kinase ATR (which responds to stalled replication) is necessary for cyclin D1 loss following genotoxic stress. We utilized $ATM^{+/+}$ or $ATM^{-/-}$ murine fibroblasts for this analysis. To facilitate detection, we expressed Flag-tagged cyclin D1 in these cells since our analysis has revealed that ectopic protein is regulated as effectively as endogenous protein (see Fig. 2). In $ATM^{-/-}$ cells, cyclin D1 levels remained elevated, while cyclin D1 was degraded in matched passage $ATM^{+/+}$ cells following stress (Fig. 5A). Consistent with ATM coordinating cyclin D1 loss, cyclin D1

phosphorylation was only induced in $ATM^{+/+}$ cells following γ IR (Fig. 5B). Furthermore, pharmacological inhibition of ATM with KU55933 also inhibited cyclin D1 phosphorylation (Fig. 5C).

Since ATM and Mre11-dependent DNA resection following DSBs will also trigger activation of ATR (27), we determined whether ATR signaling contributed to DSB-induced cyclin D1 loss. Stalled DNA replication induced by aphidicolin treatment was insufficient to induce cyclin D1 phosphorylation or degradation despite activation of Chk1, a checkpoint kinase downstream of ATR (Fig. 2G and H), suggesting that the ATR pathway does not regulate cyclin D1. The role of ATR was directly assessed using fibroblasts harboring a tamoxifen-inducible ATR allele, $ATR^{lox/-}$ (13). Cells were treated with dimethyl sulfoxide (DMSO) or 200 nM 4-OH tamoxifen (TAM) for 24 h to induce ATR deletion, followed by a 12-h incubation to allow for ATR depletion. Cyclin D1 levels were equivalent in the presence or absence of ATR after γ IR (Fig. 6A) or HU treatment (Fig. 6B). In addition, attenuation of endogenous ATR expression via ATR-specific siRNA did not alter cyclin D1 phosphorylation or degradation following γ IR, despite efficient knockdown (Fig. 6C). Taken together, these data reveal that cyclin D1 regulation following DNA damage occurs downstream of ATM activation.

Because Chk2 is a primary effector of ATM (30), we assessed whether activation of Chk2 is required for cyclin D1

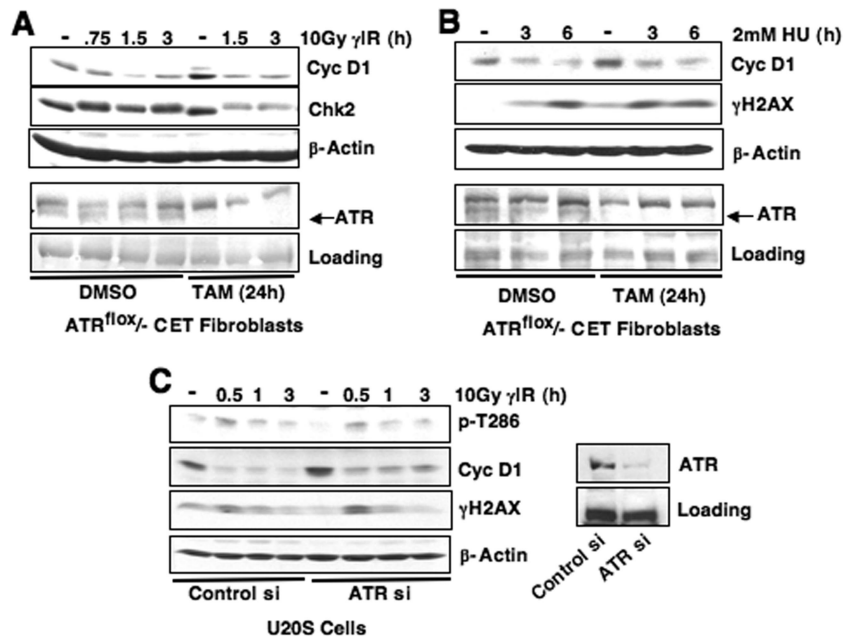


FIG. 6. ATR is dispensable for DSB-induced cyclin D1 loss. (A and B) ATR deletion does not alter cyclin D1 degradation following DNA damage. ATR^{flox/-} CET fibroblasts were treated with 4-OH tamoxifen (TAM) for 24 h, followed by incubation at 37°C for 12 h to allow sufficient ATR depletion. Cells were then irradiated (A) or treated with 2 mM HU (B) as indicated, and the cyclin D1 levels were assessed by immunoblotting. Significant ATR deletion was obtained by TAM treatment. (C) siRNA-mediated attenuation of ATR expression does not inhibit cyclin D1 phosphorylation or degradation. U2OS cells were transfected with ATR-specific siRNA and irradiated as indicated 60 h after siRNA delivery. Cyclin D1 phosphorylation and total cyclin D1 and the efficiency of ATR knockdown were assessed by immunoblotting.

loss. Knockdown of Chk2 via siRNA attenuated but did not abrogate DSB-dependent cyclin D1 destruction (Fig. 7A). We also assessed whether inhibition of Chk1, the downstream ATR effector, affects cyclin D1 phosphorylation and loss following DSB induction (Fig. 7B and C). Significantly, use of the Chk1-specific inhibitor SB218078 or attenuation of Chk1 expression via shRNA did not alter cyclin D1 phosphorylation or degradation in S-phase cells treated with HU (Fig. 7B and C, respectively). Finally, we determined whether there is synergy between Chk1 and Chk2 in regulating cyclin D1 following DSB induction. siRNA-mediated knockdown of Chk2 modestly attenuates cyclin D1 degradation at early time points in U2OS cells; in contrast, cyclin D1 levels are equivalent in control and Chk2 siRNA conditions at later time points (3 h) (Fig. 7D). Significantly, addition of a Chk1 inhibitor, SB218078, did not further stabilize cyclin D1 levels, suggesting that Chk1 and Chk2 activity is not synergistic in regulating cyclin D1 (Fig. 7D). These results suggest that Chk2 may play a role in cyclin D1 regulation; however, additional ATM-dependent effectors also function in DNA damage-induced cyclin D1 regulation. Collectively, our data support a model wherein ATM activation following DSB induction is necessary for cyclin D1 phosphorylation and subsequent degradation. However, future investigation of regulators downstream of ATM, including Chk2, is important to completely delineate the DNA damage-specific signaling network that coordinates cyclin D1 destruction.

SCF^{Fbx4- α Bcrystallin} is required for cyclin D1 degradation following DNA damage. SCF^{Fbx4- α Bcrystallin} was recently revealed to direct p-T286-dependent ubiquitylation of cyclin D1 in both fibroblasts and epithelial cells (36). Fbx4 and α B crystallin serve as substrate-specific adaptors that recognize phos-

phorylated cyclin D1. To directly assess the role of Fbx4 and α B crystallin in DNA damage-induced cyclin D1 proteolysis, we utilized NIH 3T3 cells wherein either Fbx4 or α B crystallin have been stably knocked down by shRNA (36). Knockdown of either Fbx4 or α B crystallin significantly attenuated cyclin D1 proteolysis following DNA damage (Fig. 8A and B).

Previous work revealed disruption of the α B crystallin locus in several breast cancer-derived cell lines (36). We utilized one such cell line, MDA-MB231 cells, to independently determine whether α B crystallin is required for cyclin D1 degradation following DSB induction. Consistent with the results obtained utilizing NIH 3T3 cells expressing α B crystallin shRNA, irradiation of MDA-MB231 cells did not trigger cyclin D1 loss, while reintroduction of exogenous α B crystallin restored DNA damage-induced cyclin D1 degradation (Fig. 8C, compare the 1-h and 3-h treatments in the left panel to the corresponding treatments in the right panel).

While our data reveal cyclin D1 destruction following DSB initiation to be dependent upon p-T286 and the SCF^{Fbx4- α Bcrystallin} ligase, the anaphase-promoting complex/cyclosome (APC/C) has also been implicated in the regulation of cyclin D1 degradation during G₁ phase following γ IR (1). Importantly, the cell line utilized for these studies, MCF7, lacks endogenous α B crystallin expression, thereby rendering the Fbx4 ligase inactive in these cells (36). Since cyclin D1 turns over, albeit with slower kinetics in this cell line, an alternative degradation pathway is likely. To determine whether APC/C contributes to cyclin D1 degradation in cells expressing a functional Fbx4-dependent ligase, we mutated L32 of cyclin D1 within the putative destruction box (1) to alanine and examined cyclin D1 stability following DNA damage. The D1-L32A mutant is degraded similarly to wild-type protein

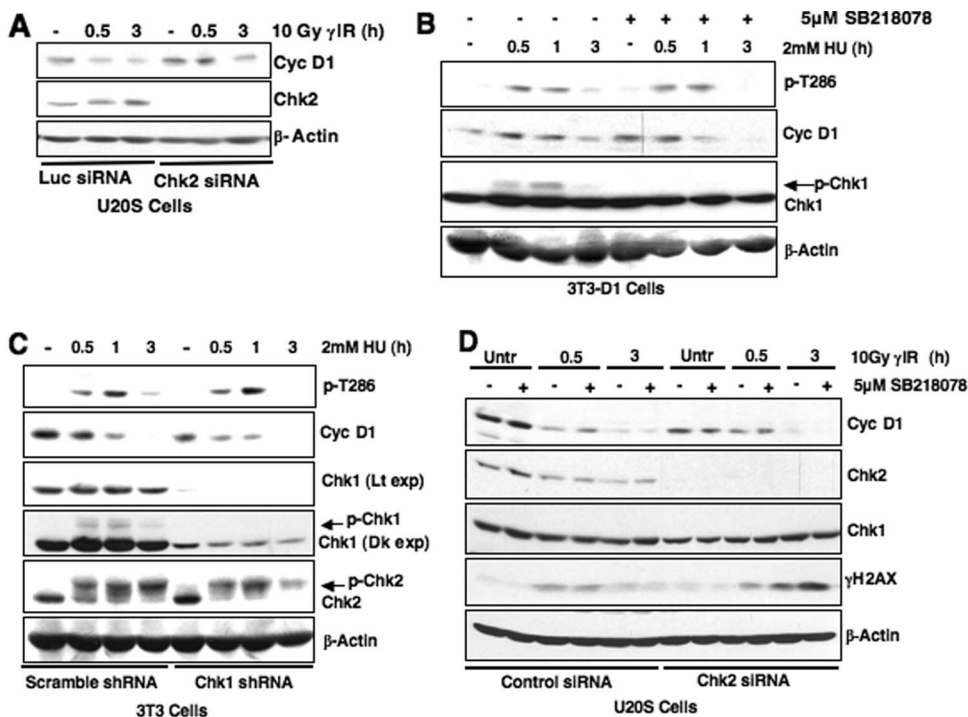


FIG. 7. Examining the role of Chk1 and Chk2 kinases in cyclin D1 regulation. (A) Chk2 knockdown modestly attenuates DNA damage-induced cyclin D1 degradation. U2OS cells were transiently transfected with Chk2-specific or luciferase control siRNAs. At 60 h posttransfection, the cells were gamma-irradiated, and cyclin D1 levels were assessed. (B and C) Chk1 activation is not required for cyclin D1 phosphorylation. Synchronous 3T3-D1 cells were pretreated with the Chk1 inhibitor SB218078 for 30 min (B), or NIH 3T3 cells were transduced with Chk1 shRNA lentivirus (C). Cells were treated with HU, and cyclin D1 phosphorylation or total protein levels were assessed by immunoblotting. (D) Chk1 and Chk2 activity is not synergistic in regulating cyclin D1. U2OS cells expressing Chk2-specific siRNA were treated with the Chk1 inhibitor SB218078. Cyclin D1 levels were assessed by immunoblotting following DNA damage.

(Fig. 8D); we also demonstrate that this mutant has impaired CDK4 binding potential, which is consistent with the disruption of residues proximal to the cyclin box (Fig. 8D). In addition, D1-L32A is degraded in MCF7 cells reconstituted with exogenous α B crystallin (data not shown), suggesting that restored SCF^{Fbx4- α Bcrystallin} ligase activity shifts cyclin D1 destruction from alternative mechanisms to the phosphorylation-dependent destruction pathway.

Recent work revealed that disruption of SCF^{Fbx4- α Bcrystallin} allows accumulation of cyclin D1 in the nucleus, and impaired ligase function results in neoplastic transformation (4). We therefore determined whether knockdown of Fbx4 sensitizes cells to chromatid breaks following DNA damage analogous to cyclin D1T286 (Fig. 1B). NIH 3T3 cells stably expressing vector control, Fbx4shRNA, or cyclin D1T286A were synchronized and treated with HU during S phase. Metaphase spreads were prepared and analyzed for chromatid breaks. In agreement with splenocytes derived from E μ -D1T286A transgenic mice, NIH 3T3 cells expressing cyclin D1T286A exhibited a significant increase in chromatid breaks following HU treatment. Analogous with cyclin D1T286A expression, knockdown of Fbx4 also results in increased chromatid breaks following HU treatment compared to the vector control (Fig. 8E and F).

Cyclin D1 stabilization compromises the intra-S-phase checkpoint. Cyclin D1 mutants refractory to ubiquitin-mediated proteolysis accumulate in the nucleus as active cyclin D1/CDK4 complexes and drive DNA rereplication (2). This deregulated

replication results from stabilization of the prereplication licensing factor Cdt1, which promotes loading of the MCM helicase (2). Cdt1 degradation in response to DNA damage is necessary to inhibit replication of damaged DNA (24, 25, 42). Since cyclin D1 is rapidly degraded following DSB induction, we considered whether failure to degrade cyclin D1 would impede Cdt1 destruction. To test this notion, we assessed Cdt1 stability following DNA damage; HeLa cells were transiently transfected with wild-type or T286A cyclin D1 constructs, along with CDK4, and treated with bleomycin. Cdt1 levels were attenuated in the presence of wild-type cyclin D1, while D1T286A-expressing cells exhibited Cdt1 stabilization up to 2 h of bleomycin treatment (Fig. 9A), a finding consistent with published results (2). Maintenance of Cdt1 should have a direct impact on MCM chromatin loading following DNA damage. We assessed chromatin retention of MCM complexes in human cancer-derived cells that express endogenous cyclin D1 wild-type or P287A. MCM3 (as a surrogate marker of MCM loading) dissociates from chromatin with a concomitant increase in soluble MCM3 protein following DNA damage in the presence of wild-type cyclin D1; however, MCM3 was stabilized on chromatin in P287A-expressing cells (Fig. 9B). PCNA serves as a representative chromatin bound protein, and loading of the chromatin fraction was also examined by Ponceau-S stain. These data suggest that improper maintenance of pre-RC components on chromatin contributes to

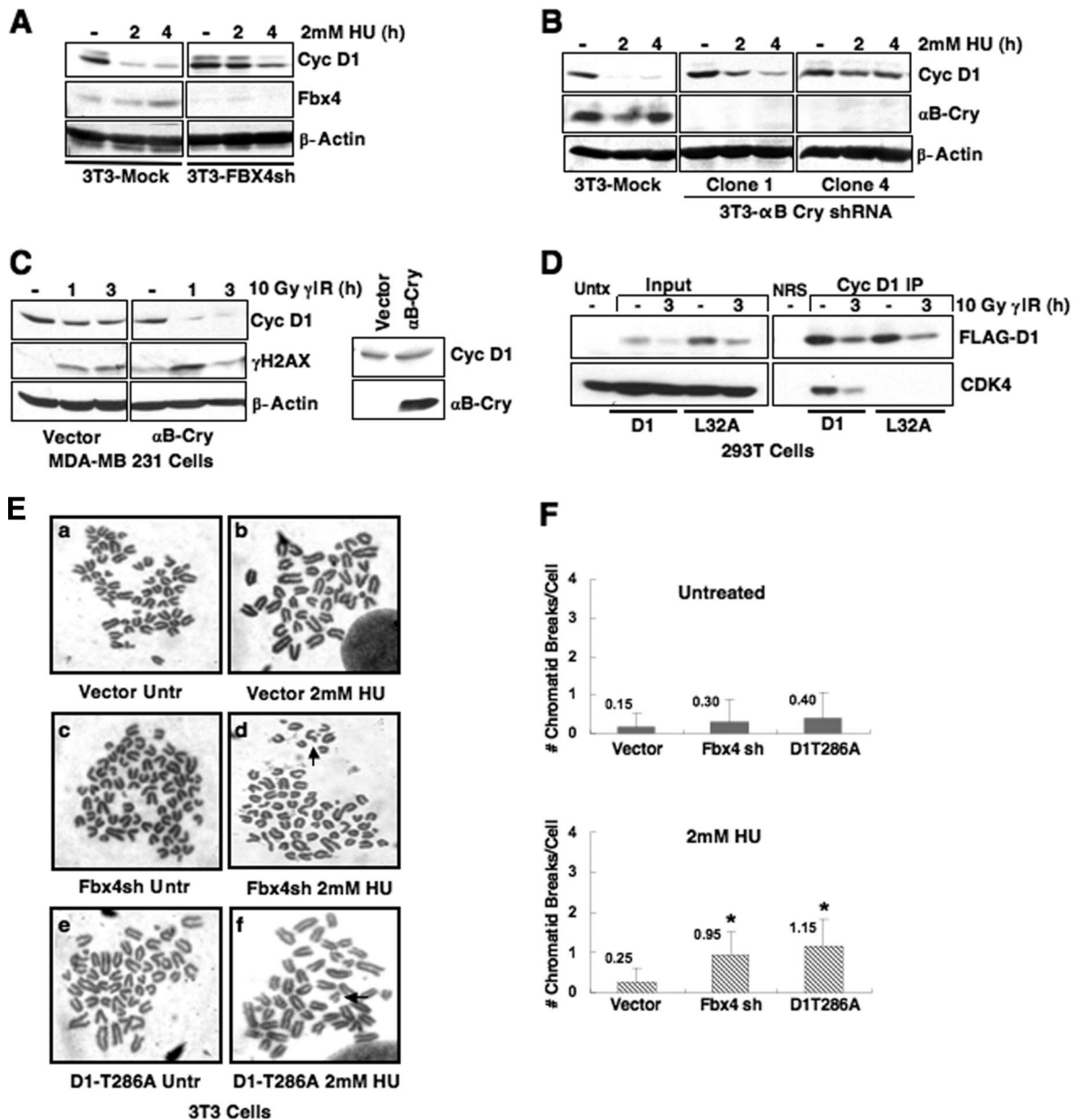


FIG. 8. The SCF^{Fbx4- α Bcrystallin} E3 ubiquitin ligase regulates cyclin D1 stability following DNA damage. Fbx4 and α B crystallin are required for efficient cyclin D1 degradation following DNA damage. (A and B) Synchronous NIH 3T3 cells stably expressing control and either Fbx4 (A) or α B crystallin-specific shRNAs (B) were treated with 2 mM HU, and cell lysates were probed for Fbx4 (A) or α B crystallin (B) to confirm knockdown and cyclin D1 to assess protein stability following DNA damage. (C) Asynchronous MDA-MB231 cells expressing empty vector or α B crystallin were γ -irradiated, followed by recovery at 37°C, and cyclin D1 stability was assessed by immunoblotting. Confirmation of exogenous α B crystallin expression in this cell line is shown. (D) Mutation of leucine 32 within the RxxL motif does not alter DNA damage-induced cyclin D1 degradation. 293T cells (chosen for high transfection efficiency and expression of SCF-Fbx4 ligase components) were transfected with Flag-tagged wild-type or D1L32A, along with CDK4 and GFP. Cell lysates were prepared and precipitated with M2 agarose beads to recognize Flag-tagged protein. Immunoprecipitates and input Western blots were probed with cyclin D1 and CDK4 antibodies to assess cyclin D1 and CDK4 association. (E) Disruption of SCF^{Fbx4- α Bcrystallin} sensitizes cells to genomic instability after HU treatment. NIH 3T3 cells stably expressing vector control or Fbx4-specific shRNA were treated with 2 mM HU for 3 h, followed by nocodazole treatment to arrest cells in metaphase. Cells were fixed, and metaphase spreads were prepared. Representative images of chromatid breaks are shown (E), and the average number of chromatid breaks per spread was quantified for each treatment (F). NIH 3T3 cells stably expressing cyclin D1T286A served as a positive control for the presence of chromatid breaks following HU.

cyclin D1T286A-driven perturbations in DNA replication, a finding consistent with previously published reports (2).

To directly determine whether cyclin D1 stabilization overrides the intra-S-phase checkpoint, we assessed RDS in cells

expressing equivalent steady-state levels (prior to DNA damage) of either wild-type cyclin D1 or D1T286A (Fig. 2E). DNA synthesis decreases significantly following γ IR in naive 3T3 and 3T3-D1 cells ($P < 0.05$). However, DNA synthesis was not

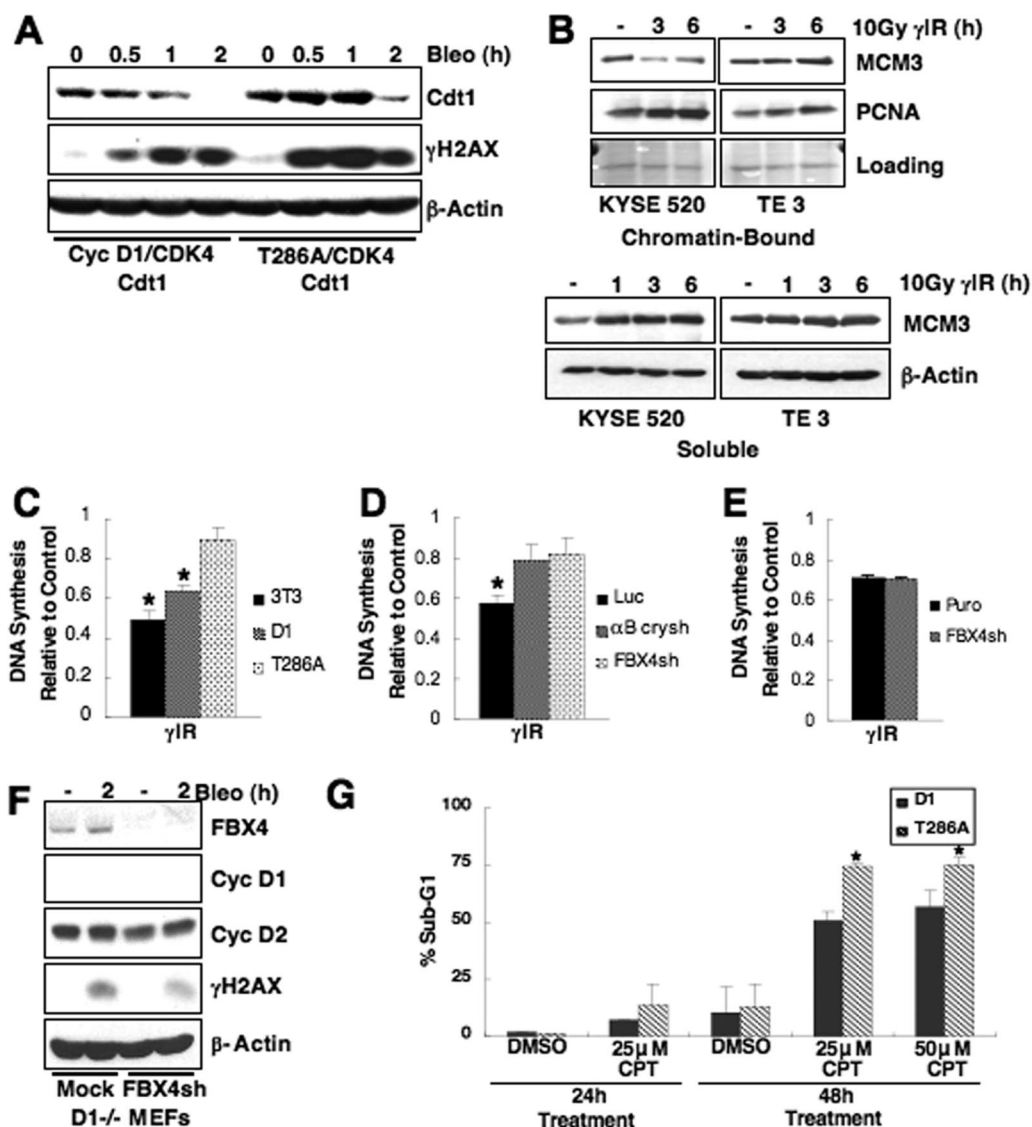


FIG. 9. Failure to degrade cyclin D1 compromises the intra-S-phase checkpoint response to DNA damage and sensitizes cells to CPT. (A) The replication factor Cdt1 is stabilized following DNA damage in cells expressing cyclin D1T286A. HeLa cells were transfected with wild-type or cyclin D1T286A, CDK4, and Cdt1. Cells were treated with 10 μ g of bleomycin/ml as indicated, and Cdt1 levels were assessed by immunoblotting. (B) Cyclin D1 stabilization promotes maintenance of MCM proteins on chromatin. Esophageal carcinoma cell lines expressing endogenous wild-type or D1P287A were irradiated and harvested at the time points indicated. Cell lysates were fractionated into chromatin-bound and soluble fractions; MCM3 binding to chromatin was assessed by immunoblotting on chromatin-bound fractions. Ponceau-S stain served as a control for equal loading of chromatin-bound fractions, and PCNA is a representative chromatin-bound protein. (C) Expression of D1T286A results in RDS. RDS assays were performed in synchronous parental NIH 3T3 cells or 3T3-D1 or 3T3-D1T286A cells. Equal concentrations of DNA were counted for [3 H] and [14 C]thymidine incorporation. DNA synthesis, calculated as the ratio of [3 H] to [14 C], was normalized to the nonirradiated control for each cell line. (D) Disruption of SCF^{Fbx4- α Bcrystallin} promotes RDS. RDS assays were performed as in panel C utilizing cells stably expressing luciferase, α B crystallin, or Fbx4-specific shRNA. (E) Fbx4 attenuation in cyclin D1-null cells does not result in RDS. RDS assays as in panel C were performed in wild-type or cyclin D1-null MEFs stably expressing empty vector or Fbx4-specific shRNAs. (F) Fbx4 levels are attenuated in cyclin D1-null MEFs stably expressing Fbx4-specific shRNA. (G) Failure to degrade cyclin D1 sensitizes cells to the CPT. 3T3-D1 or D1T286A cells were treated with CPT as indicated for 24 or 48 h. Cells were fixed and stained with propidium iodide and subjected to FACS analysis; a sub-G₁ population is indicative of apoptotic cells.

significantly decreased in D1T286A-expressing cells (Fig. 9C). We also measured RDS in NIH 3T3 cells where Fbx4 levels are reduced through shRNA technology. Analogous with degradation-refractory D1T286A, knockdown of Fbx4 or α B crystallin promoted RDS (Fig. 9D). In contrast, knockdown of Fbx4 in cyclin D1^{-/-} fibroblasts failed to trigger RDS (Fig. 9E and F), which is consistent with cyclin D1 as the primary regulatory

target of Fbx4 pertaining to cell cycle progression. Although RDS is often associated with a failure of cells to inhibit CDK2, our analysis revealed effective inhibition of CDK2 kinase in D1T286A-expressing cells (data not shown), suggesting that the maintenance of cyclin D1/CDK4 activity directly contributes to the RDS phenotype.

Since cyclin D1T286A expression promotes RDS, we hy-

pothesized that cells expressing stabilized cyclin D1 would be sensitized to the S-phase-specific CPT. To address this hypothesis, 3T3-D1 or 3T3-D1T286A cells were treated with 25 or 50 μ M CPT for 24 or 48 h; cells were harvested, stained with propidium iodide, and subjected to FACS analysis to determine cell cycle distribution. A significant increase in sub-G₁ cells was observed after CPT treatment for 48 h ($P < 0.05$), providing evidence that cyclin D1T286A-expressing cells are sensitized to CPT (Fig. 9G). Taken together, the RDS phenotype and S-phase chemotherapy sensitivity observed in D1T286A-expressing cells highlights a potential therapeutic strategy for tumors exhibiting stabilized cyclin D1.

DISCUSSION

Recent work has revealed that alterations in posttranslational control of cyclin D1 contribute to neoplastic growth in model systems and in human cancers (4, 11, 21, 36). Cyclin D1 accumulation in the nuclear compartment, where it functions as an allosteric activator of CDK4, contributes directly to G₁ progression and cell proliferation. Importantly, accumulation is limited by ubiquitin-mediated proteolysis catalyzed by SCF^{Fbx4- α Bcrystallin}, and loss of proteolytic control contributes to neoplastic growth (18, 36). The findings presented here reveal that nuclear stabilization of cyclin D1 compromises the intra-S-phase checkpoint following DNA damage. While cyclin D1 is an inherently unstable protein, genotoxic stress further accelerates its proteolysis in a manner that depends upon GSK3 β -mediated p-T286 and ubiquitylation by the SCF^{Fbx4- α Bcrystallin} E3 ligase. Mutations that impair cyclin D1 phosphorylation or inactivate SCF^{Fbx4- α Bcrystallin} result in the accumulation of active cyclin D1/CDK4 in the nucleus, which in turn impairs checkpoint-dependent inhibition of DNA replication. Ultimately, the ensuing RDS results in the accumulation of chromatid breaks.

Thr-286 phosphorylation is required for both cell cycle- and DNA damage-mediated destruction of cyclin D1. Although additional kinases have been implicated as regulators of p-T286 (15, 33, 43), our data provide strong evidence for GSK3 β as the Thr-286 kinase. GSK3 β inhibition via LiCl treatment enriches nuclear cyclin D1 (3); LiCl, a small molecule GSK3 β inhibitor (SB216763), kdGSK3 β , and shRNA all significantly attenuate DNA damage-induced Thr-286 phosphorylation. Importantly, inhibition of the two additional kinases implicated as regulators of cyclin D1, IKK α (data not shown) and p38 (Fig. 4G), had no effect on cyclin D1 phosphorylation or degradation in response to DSB induction.

GSK3 β contributes directly to cyclin D1 regulation in multiple ways. First, phosphorylation of Thr-286 is required for CRM1-mediated nuclear export (3). Second, phosphorylated cyclin D1 is recognized by Fbx4, the specificity factor for the SCF E3 ligase, once relocalized to the cytoplasm (36). Our data reveal that shRNA-mediated reduction of either Fbx4 or α B crystallin stabilizes cyclin D1 in the presence of DSBs. Consistently, cyclin D1 is also refractory to DNA damage-dependent degradation in breast cancer cells lacking endogenous α B crystallin expression, while reintroduction of exogenous α B crystallin restores cyclin D1 turnover. Collectively, these data support a model wherein upregulation of GSK3 β -dependent cyclin D1 phosphorylation following genotoxic

stress targets the protein for SCF^{Fbx4- α Bcrystallin}-mediated destruction.

Previous work implicated the APC/C in DNA damage-induced cyclin D1 degradation (1). A putative RxxL destruction box in the N terminus of cyclin D1 was identified as being responsible for directing APC/C-dependent degradation. Our work reveals that mutation of Thr-286, loss of Fbx4, or inhibition of GSK3 β impairs DSB-mediated cyclin D1 loss; we also assessed the potential contribution of the RxxL motif. Leucine 32-to-alanine (L32A) mutation did not impair DSB-induced loss. Importantly, this mutation profoundly impairs CDK4 binding, most likely resulting from disruption of protein structure just proximal to the cyclin box. Thus, alterations in folding of this mutant could contribute to its stabilization under some conditions.

While mutations near the cyclin box clearly alter structural interactions with CDK4, this may not be the only reason accounting for discrepancies regarding the role of different E3 ligases in cyclin destruction. An additional possibility is that this previous work utilized MCF7 cells, a cell line lacking α B crystallin (36), thereby inactivating the SCF^{Fbx4- α Bcrystallin} ubiquitin ligase. While cyclin D1 proteolysis is significantly attenuated in these cells, restoration of α B crystallin rescues both mitogen and DSB-dependent cyclin D1 proteolysis (data not shown). A third E3 ligase utilizing Fbw8 as a specificity cofactor has been implicated in regulating cyclin D1 (43). We have not assessed Fbw8 directly due to a lack of suitable antibodies and cannot rule out its potential role in regulating D1. However, Cul7, a core component of the Fbw8 ligase, is undetectable in NIH 3T3 cells (29), and our data revealing that knockdown of either Fbx4 or α B crystallin is sufficient to inhibit cyclin D1 proteolysis emphasizes their requisite role in this regulatory process.

During S phase, DNA must be replicated with high fidelity to ensure error-free propagation of genetic material. DSBs resulting from various stresses invoke a checkpoint that attenuates cell cycle progression until DNA is repaired (6). The intra-S-phase checkpoint is characterized by replication fork stalling, inhibition of origin firing, and accumulation of single-strand DNA, promoting ATR activation; in contrast, the accumulation of DSBs, regardless of replication status, triggers ATM activation (6, 30). Strikingly, inhibition of cyclin D1 degradation impairs checkpoint response, and cells exhibit an RDS phenotype, implying checkpoint failure. The RDS phenotype observed in cyclin D1T286A-expressing cells is accompanied by Cdt1 stabilization, which is dependent upon CDK4 activation by cyclin D1. Ultimately, the continued presence of Cdt1 contributes to retention of MCM helicase on chromatin, suggesting that the presence of this mutant within the nucleus perturbs pre-RC disassembly following DNA damage. The significance of the cyclin D1T286A RDS phenotype is highlighted by increased presence of chromatid breaks in primary splenocytes treated with DNA-damaging agents.

While the ability of constitutively nuclear D1T286A to promote CDT1 stabilization is clear, how does inactivation of the Fbx4 ligase in cells harboring wild-type cyclin D1 equate with the same biochemical function? Importantly, published work reveals that inactivation of SCF^{Fbx4- α Bcrystallin} results in the nuclear accumulation of endogenous cyclin D1/CDK4 kinase, leading to Cdt1 stabilization and function in both cycling cells

and following DSB generation (4, 2). Accordingly, our data are consistent with these findings and further reveal the retention of MCM on chromatin following DSBs. In addition, shRNA-mediated attenuation of Fbx4 expression promotes an RDS phenotype that correlates with increased genomic instability following treatment with DNA-damaging agents.

Previous work suggested that inhibition of cyclin D1/CDK4 activity is critical for genotoxic stress induced cell cycle arrest (1). Significantly, cyclin D1-driven DNA rereplication requires CDK4 kinase activity (2). Our findings here not only reveal the molecular nature of the ligase that regulates cyclin D1 but also importantly provide mechanistic insight with regard to the consequences of the accumulation of stabilized cyclin D1 and thus cyclin D1/CDK4 kinase. In the absence of CDK4 kinase, premalignant cells could successfully halt DNA replication, thereby reducing genomic instability that may promote transformation.

Given the RDS phenotype associated with maintenance of cyclin D1 protein following genotoxic stress, it is not surprising that ATM signaling is required to coordinate cyclin D1 destruction. Consistent with our model of DSB induction as a prerequisite for cyclin D1 phosphorylation and destruction, the accumulation of single-strand DNA and subsequent ATR activation is insufficient to direct cyclin D1 loss. Significantly, damage-induced cyclin D1 phosphorylation and destruction are abrogated in ATM-null cells, and use of an ATM-specific inhibitor dramatically attenuates cyclin D1 phosphorylation. However, it is possible that ATR could contribute to ATM activation following fork stalling (47). The fact that ATR depletion did not attenuate cyclin D1 phosphorylation/degradation and that cyclin D1 is not phosphorylated following stress that does not trigger DSB implies that cyclin D1 loss is ATM dependent and ATR independent.

While ATM is required for DNA damage-induced cyclin D1 phosphorylation, the precise effector-signaling network remains unclear. Chk2 appears to function in the regulation of cyclin D1 degradation at early time points following γ IR; however, Chk2 knockdown and/or inhibition fails to rescue cyclin D1 degradation at later time points after damage. As loss of ATM and GSK3 β functions to stabilize cyclin D1 at all time points, this result suggests an alternative ATM effector in the mediation of GSK3 β -dependent cyclin D1 degradation. Delineating the molecular signaling network connecting ATM with cyclin D1 Thr-286 phosphorylation is an exciting area for future study.

ACKNOWLEDGMENTS

We thank P. Sicinski for the D1^{-/-} fibroblasts and Roger Greenberg for control and Chk2 siRNA.

This study was supported by CA93237 (National Institutes of Health) and a Leukemia and Lymphoma Scholar award (J.A.D.) and the Pew Foundation in the Biomedical Sciences and the Department of Pathology of the Children's Hospital of Philadelphia (C.H.B.).

REFERENCES

1. Agami, R., and R. Bernards. 2000. Distinct initiation and maintenance mechanisms cooperate to induce G₁ cell cycle arrest in response to DNA damage. *Cell* **102**:55–66.
2. Aggarwal, P., M. D. Lessie, D. I. Lin, L. Pontano, A. B. Gladden, B. Nuskey, A. Goradia, M. A. Wasik, A. J. Klein-Szanto, A. K. Rustgi, C. H. Bassing, and J. A. Diehl. 2007. Nuclear accumulation of cyclin D1 during S phase inhibits Cul4-dependent Cdt1 proteolysis and triggers p53-dependent DNA rereplication. *Genes Dev.* **21**:2908–2922.
3. Alt, J. R., J. L. Cleveland, M. Hannink, and J. A. Diehl. 2000. Phosphorylation-dependent regulation of cyclin D1 nuclear export and cyclin D1-dependent cellular transformation. *Genes Dev.* **14**:3102–3114.
4. Barbash, O., P. Zamfirova, D. I. Lin, X. Chen, K. Yang, H. Nakagawa, F. Lu, A. K. Rustgi, and J. A. Diehl. 2008. Mutations in Fbx4 inhibit dimerization of the SCF(Fbx4) ligase and contribute to cyclin D1 overexpression in human cancer. *Cancer Cell* **14**:68–78.
5. Barnes, D. M., and C. E. Gillett. 1998. Cyclin D1 in breast cancer. *Breast Cancer Res. Treat.* **52**:1–15.
6. Bartek, J., C. Lukas, and J. Lukas. 2004. Checking on DNA damage in S phase. *Nat. Rev. Mol. Cell. Biol.* **5**:792–804.
7. Bartkova, J., J. Lukas, H. Muller, D. Lutzhoft, M. Strauss, and J. Bartek. 1994. Cyclin D1 protein expression and function in human breast cancer. *Int. J. Cancer* **57**:353–361.
8. Bartkova, J., J. Lukas, H. Muller, M. Strauss, B. Gusterson, and J. Bartek. 1995. Abnormal patterns of D-type cyclin expression and G₁ regulation in human head and neck cancer. *Cancer Res.* **55**:949–956.
9. Bartkova, J., J. Lukas, M. Strauss, and J. Bartek. 1994. The PRAD-1/cyclin D1 oncogene product accumulates aberrantly in a subset of colorectal carcinomas. *Int. J. Cancer* **58**:568–573.
10. Benzeno, S., and J. A. Diehl. 2004. C-terminal sequences direct cyclin D1-CRM1 binding. *J. Biol. Chem.* **279**:56061–56066.
11. Benzeno, S., F. Lu, M. Guo, O. Barbash, F. Zhang, J. G. Herman, P. S. Klein, A. Rustgi, and J. A. Diehl. 2006. Identification of mutations that disrupt phosphorylation-dependent nuclear export of cyclin D1. *Oncogene* **25**:6291–6303.
12. Bianchi, V., E. Pontis, and P. Reichard. 1986. Changes of deoxyribonucleoside triphosphate pools induced by hydroxyurea and their relation to DNA synthesis. *J. Biol. Chem.* **261**:16037–16042.
13. Brown, E. J., and D. Baltimore. 2003. Essential and dispensable roles of ATR in cell cycle arrest and genome maintenance. *Genes Dev.* **17**:615–628.
14. Calbo, J., M. Parreno, E. Sotillo, T. Yong, A. Mazo, J. Garriga, and X. Grana. 2002. G₁ cyclin/cyclin-dependent kinase-coordinated phosphorylation of endogenous pocket proteins differentially regulates their interactions with E2F4 and E2F1 and gene expression. *J. Biol. Chem.* **277**:50263–50274.
15. Casanovas, O., F. Miro, J. M. Estanyol, E. Itarte, N. Agell, and O. Bachs. 2000. Osmotic stress regulates the stability of cyclin D1 in a p38SAPK2-dependent manner. *J. Biol. Chem.* **275**:35091–35097.
16. Costanzo, V., K. Robertson, C. Y. Ying, E. Kim, E. Avvedimento, M. Gottesman, D. Grieco, and J. Gautier. 2000. Reconstitution of an ATM-dependent checkpoint that inhibits chromosomal DNA replication following DNA damage. *Mol. Cell* **6**:649–659.
17. Diehl, J. A., M. Cheng, M. F. Roussel, and C. J. Sherr. 1998. Glycogen synthase kinase-3 β regulates cyclin D1 proteolysis and subcellular localization. *Genes Dev.* **12**:3499–3511.
18. Diehl, J. A., F. Zindy, and C. J. Sherr. 1997. Inhibition of cyclin D1 phosphorylation on threonine-286 prevents its rapid degradation via the ubiquitin-proteasome pathway. *Genes Dev.* **11**:957–972.
19. Falck, J., J. H. Petrini, B. R. Williams, J. Lukas, and J. Bartek. 2002. The DNA damage-dependent intra-S phase checkpoint is regulated by parallel pathways. *Nat. Genet.* **30**:290–294.
20. Gladden, A. B., and J. A. Diehl. 2003. The cyclin D1-dependent kinase associates with the pre-replication complex and modulates RB/MCM7 binding. *J. Biol. Chem.* **278**:9754–9760.
21. Gladden, A. B., R. Woolery, P. Aggarwal, M. A. Wasik, and J. A. Diehl. 2006. Expression of constitutively nuclear cyclin D1 in murine lymphocytes induces B-cell lymphoma. *Oncogene* **25**:998–1007.
22. Harbour, J. W., R. X. Luo, A. Dei Santi, A. A. Postigo, and D. C. Dean. 1999. Cdk phosphorylation triggers sequential intramolecular interactions that progressively block Rb functions as cells move through G₁. *Cell* **98**:859–869.
23. Hatakeyama, M., J. A. Brill, G. R. Fink, and R. A. Weinberg. 1994. Collaboration of G₁ cyclins in the functional inactivation of the retinoblastoma protein. *Genes Dev.* **8**:1759–1771.
24. Higa, L. A., I. S. Mihaylov, D. P. Banks, J. Zheng, and H. Zhang. 2003. Radiation-mediated proteolysis of CDT1 by CUL4-ROC1 and CSN complexes constitutes a new checkpoint. *Nat. Cell Biol.* **5**:1008–1015.
25. Hu, J., C. M. McCall, T. Ohta, and Y. Xiong. 2004. Targeted ubiquitination of CDT1 by the DDB1-CUL4A-ROC1 ligase in response to DNA damage. *Nat. Cell Biol.* **6**:1003–1009.
26. Ikeguchi, M., T. Sakatani, T. Ueta, and N. Kaibara. 2001. Cyclin D1 expression and retinoblastoma gene protein (pRB) expression in esophageal squamous cell carcinoma. *J. Cancer Res. Clin. Oncol.* **127**:531–536.
27. Jazayeri, A., J. Falck, C. Lukas, J. Bartek, G. C. Smith, J. Lukas, and S. P. Jackson. 2006. ATM- and cell cycle-dependent regulation of ATR in response to DNA double-strand breaks. *Nat. Cell Biol.* **8**:37–45.
28. Jin, M., S. Inoue, T. Umemura, J. Moriya, M. Arakawa, K. Nagashima, and H. Kato. 2001. Cyclin D1, p16 and retinoblastoma gene product expression as a predictor for prognosis in non-small cell lung cancer at stages I and II. *Lung Cancer* **34**:207–218.
29. Kasper, J. S., H. Kuwabara, T. Arai, S. H. Ali, and J. A. DeCaprio. 2005.

- Simian virus 40 large T antigen's association with the CUL7 SCF complex contributes to cellular transformation. *J. Virol.* **79**:11685–11692.
30. **Kastan, M. B., and J. Bartek.** 2004. Cell-cycle checkpoints and cancer. *Nature* **432**:316–323.
 31. **Khanna, K. K., and S. P. Jackson.** 2001. DNA double-strand breaks: signaling, repair, and the cancer connection. *Nat. Genet.* **27**:247–254.
 32. **Kida, A., K. Kakhana, S. Kotani, T. Kurosu, and O. Miura.** 2007. Glycogen synthase kinase-3 β and p38 phosphorylate cyclin D2 on Thr280 to trigger its ubiquitin/proteasome-dependent degradation in hematopoietic cells. *Oncogene* **26**:6630–6640.
 33. **Kwak, Y. T., R. Li, C. R. Becerra, D. Tripathy, E. P. Frenkel, and U. N. Verma.** 2005. I κ B kinase alpha regulates subcellular distribution and turnover of cyclin D1 by phosphorylation. *J. Biol. Chem.* **280**:33945–33952.
 34. **Lee, J. Y., S. J. Yu, Y. G. Park, J. Kim, and J. Sohn.** 2007. Glycogen synthase kinase 3 β phosphorylates p21WAF1/CIP1 for proteasomal degradation after UV irradiation. *Mol. Cell. Biol.* **27**:3187–3198.
 35. **Leng, X., M. Noble, P. D. Adams, J. Qin, and J. W. Harper.** 2002. Reversal of growth suppression by p107 via direct phosphorylation by cyclin D1/cyclin-dependent kinase 4. *Mol. Cell. Biol.* **22**:2242–2254.
 36. **Lin, D. I., O. Barbash, K. G. Kumar, J. D. Weber, J. W. Harper, A. J. Klein-Szanto, A. Rustgi, S. Y. Fuchs, and J. A. Diehl.** 2006. Phosphorylation-dependent ubiquitination of cyclin D1 by the SCF(FBX4- α B crystallin) complex. *Mol. Cell* **24**:355–366.
 37. **Lin, D. I., M. D. Lessie, A. B. Gladden, C. H. Bassing, K. U. Wagner, and J. A. Diehl.** 2007. Disruption of cyclin D1 nuclear export and proteolysis accelerates mammary carcinogenesis. *Oncogene* **27**:1231–1242.
 38. **Liu, J. S., S. R. Kuo, and T. Melendy.** 2003. Comparison of checkpoint responses triggered by DNA polymerase inhibition versus DNA damaging agents. *Mutat. Res.* **532**:215–226.
 39. **Lundin, C., K. Erixon, C. Arnaudeau, N. Schultz, D. Jenssen, M. Meuth, and T. Helleday.** 2002. Different roles for nonhomologous end joining and homologous recombination following replication arrest in mammalian cells. *Mol. Cell. Biol.* **22**:5869–5878.
 40. **Matsushime, H., M. F. Roussel, R. A. Ashmun, and C. J. Sherr.** 1991. Colony-stimulating factor 1 regulates novel cyclins during the G₁ phase of the cell cycle. *Cell* **65**:701–713.
 41. **Moreno-Bueno, G., S. Rodriguez-Perales, C. Sanchez-Estevéz, D. Hardisson, D. Sarrio, J. Prat, J. C. Cigudosa, X. Matias-Guiu, and J. Palacios.** 2003. Cyclin D1 gene (CCND1) mutations in endometrial cancer. *Oncogene* **22**:6115–6118.
 42. **Nishitani, H., N. Sugimoto, V. Roukos, Y. Nakanishi, M. Saijo, C. Obuse, T. Tsurimoto, K. I. Nakayama, K. Nakayama, M. Fujita, Z. Lygerou, and T. Nishimoto.** 2006. Two E3 ubiquitin ligases, SCF-Skp2 and DDB1-Cul4, target human Cdt1 for proteolysis. *EMBO J.* **25**:1126–1136.
 43. **Okabe, H., S. H. Lee, J. Phuchareon, D. G. Albertson, F. McCormick, and O. Tetsu.** 2006. A critical role for FBXW8 and MAPK in cyclin D1 degradation and cancer cell proliferation. *PLoS ONE* **1**:e128.
 44. **Raman, M., S. Earnest, K. Zhang, Y. Zhao, and M. H. Cobb.** 2007. TAO kinases mediate activation of p38 in response to DNA damage. *EMBO J.* **26**:2005–2014.
 45. **Sherr, C. J.** 1996. Cancer cell cycles. *Science* **274**:1672–1677.
 46. **Stambolic, V., L. Ruel, and J. R. Woodgett.** 1996. Lithium inhibits glycogen synthase kinase-3 activity and mimics wingless signalling in intact cells. *Curr. Biol.* **6**:1664–1668.
 47. **Stiff, T., S. A. Walker, K. Cerosaletti, A. A. Goodarzi, E. Petermann, P. Concannon, M. O'Driscoll, and P. A. Jeggo.** 2006. ATR-dependent phosphorylation and activation of ATM in response to UV treatment or replication fork stalling. *EMBO J.* **25**:5775–5782.